Degradation of Dicarboxylic Acids (C₂-C₉) upon Liquid-Phase Reactions with O₃ and Its Atmospheric Implications

OLEG V. NEPOTCHATYKH AND PARISA A. ARIYA

Aerosols are considered major players in climate change and represent health hazards. Dicarboxylic acids are among a major class of components that form secondary organic atmospheric aerosols. To understand the atmospheric transformation of these compounds, kinetic studies on the ozonolysis and the photoinduced ozonolysis ($\lambda \geq 250$ nm) of aqueous solutions of seven (C₂-C₉) dicarboxylic acids, which have been identified in atmospheric aerosols, were performed using Fourier transform infrared and ultraviolet−visible spectroscopy. The measured apparent rate constants for dicarboxylic acids in 0.1 mol L^{-1} aqueous solutions at 298 ± 2 K are as follows: oxalic, $(2.7\pm0.1)\times10^{-2}$; malonic, (5.5 ± 0.1); succinic $(6.7\pm0.4) \times 10^{-4}$; glutaric $(1.3\pm0.2)) \times 10^{-3}$; adipic $(1.7\pm0.1)) \times 10^{-3}$; pimelic $(4.4\pm0.1)) \times 10^{-3}$ and picnic, $(2.5\pm0.1)) \times 10^{-2}$ (Lmol^{-1}s^{-1}). An empirical equation is provided to estimate the ozonolysis rate constant of dicarboxylic acids containing more than three carbon atoms for which no experimental data exists. A mechanism for malonic acid ozonolysis, which explains its fast ozonolysis rate constant, is also suggested. The implications of our results to atmospheric chemistry indicate that ozonolysis and photoinduced ozonolysis are not significant removal pathways for dicarboxylic acids.

Introduction

Organic compounds form up to 50% of the total atmospheric aerosol mass and have a significant impact on geophysical, health, and environ mental issues, ranging from local scale such as pollution to global scale including climate change (e.g., refs *1* and *2*). The aerosols interact with sunlight and act as cloud condensation nuclei, subsequently altering the climate. The products of the photooxidation of biogenic or anthropogenic volatile organic compounds (VOC) can have low volatility and hence exist as condensed matter. These products form secondary organic aerosols.

Secondary aerosols are normally smaller than primary aerosol particles and are thus longer lived species. Atmospheric oxidants such as the hydroxyl radical, ozone, and the nitrate radical may react with organic molecules and form products with low vapor pressures (*2−7*). Various products were identified in secondary organic aerosols (*2, 5−7*) including oxocarboxylic acids ($OCH-R-COOH$), hydroxy- carboxylic acids ($HOCH-R-COOH$), hydroxyketocarboxylic acids ($HOCH-R_1-CO-R_2-COOH$), and dicarboxylic acids ($HOOC-R-COOH$), where R is a hydrocarbon chain (i.e. R can be $-CH_2-$, $-C_2H_4-$, etc.). Of all the identified organic acids, dicarboxylic acids have a primary importance in aerosol formation due to their extremely low vapor pressure and high hygroscopicity (*8, 9*). According to the photochemical smog com pound analysis (*6*) and laboratory experiments, dicarboxylic acids are the most abundant class of condensed- phase com pounds identified from the ozonolysis products of terpenes and other cyclic alkenes (*8, 10, 11*).

The dicarboxylic acids observed in the atmosphere include malonic, succinic, glutaric, adipic, and pinic acids (*1−3, 5−8*). Relatively short (C$_3$−C$_6$) dicarboxylic acids were found in the urban aerosols. They are believed to be the oxidation products of mostly anthropogenic VOCs (*5, 6*). Whereas, longer chain dicarboxylic acids (i.e. C$_n$ H$_{2n-2}$O$_4$; $n{\geq}5$) such as pinic, pimelic, and sabinic acids are found to be abundant in continental remote forest areas and are assumed to be the products of the photooxidation and ozonolysis of biogenic VOCs (*2, 3*). A series of C₂−C₁₁ dicarboxylic acid has been detected in equatorial and Antarctic regions (*12−15*). The most abundant dicarboxylic acids detected contained two to five carbons (C₂−C₅) and in Antarctic aerosols, C $_6$ dicarboxylic acids also dominated.

Organic aerosols absorb a considerable amount of water (*16, 17*) depending on air humidity and aerosol composition. Dicarboxylic acids become important in the formation and growth of clouds and fog due to their large hygroscopicity. Numerous studies have been performed to detect dicarboxylic acids in the atmosphere and determine their formation and aggregation patterns (*1−15*). However, their atmospheric chemical transformations have yet to be determined.

To understand the atmospheric degradation pathways of dicarboxylic acids, a liquid-phase kinetic study of the ozonolysis and the UV-induced ozonolysis of selected dicarboxylic acids was performed, under near atmospheric conditions, using Fourier transform infrared coupled to Raman (FT-IR-Raman) and ultraviolet−visible (UV−vis) spectroscopy. We herein compared the contributions of ozonolysis and photoinduced ozonolysis of dicarboxylic acid aerosols in atmosphere.

Experimental Section

We performed kinetic studies by monitoring the reactant concentrations-dicarboxylic acids and ozone. The decay of ozone in excess dicarboxylic acid solutions was followed using UV spectrophotometry (Varian Cary 50-Bio UV −vis spectrophotometer). The dicarboxylic acid concentration decay was monitored using a flow-cell coupled with FT-IR spectrometer (FT-IR-Raman spectrometer, model IMZ 9497 Bomem) at constant ozone concentration. Figure 1 represents a schematic of the experimental setup.

A 20 mL Pyrex reactor was made to carry out the ozonolysis of selected dicarboxylic acids. This chamber was equipped with four quartz windows placed at 90 ⬜ to each other, forming two perpendicular optical pathways through the reaction mixture. The reactor temperature was kept constant at 298 ± 2 K. The reactor was placed in the UV −vis spectrophotometer chamber and was aligned to directly measure ozone concentration. In selected experiments, the reactor content was irradiated with UV light ($\lambda \geq 250$ n m) using a

100 W Hg arc lamp (Oriel 6281) through high-grade quartz fiber optic bundle (77578 Oriel), which was equipped with a quartz collimating beam probe (77640 Oriel). The light beam, coming out of the collimating beam probe, was directed into the reactor through
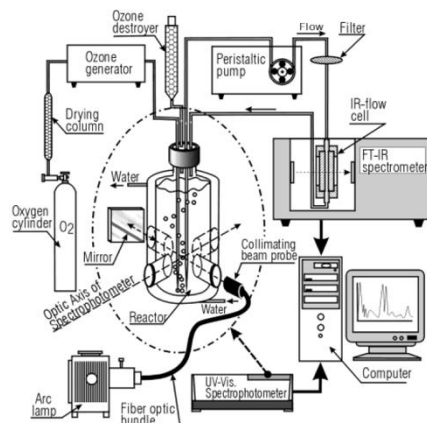

FIGURE 1. Diagram of experimental setup.

the reactor quartz window, perpendicular to the spectrometer optical axis.

Ozone produced by an ozone generator (model OL100 / DC, Ozone Services Inc.) was introduced into the reactor through a capillary tube. Decay of ozone concentration in selected experiments was registered immediately after the interruption of O_3 / O_2 flow through the reaction solution. The ozone concentration in the reaction solutions was monitored according to UV absorption of dissolved ozone in the region of $240 < \lambda < 310$ n m. Dicarboxylic acids decay was monitored continuously upon the introduction of ozone into reaction mixture using a homemade IR flow cell (construction materials: Teflon and quartz windows) in- stalled in the FT-IR-Raman spectrometer and was connected to the original ozonolysis reactor by a Teflon capillary tubing.

A peristaltic pump (model "Simon" Manostat, Barnald) allowed for the circulation of the liquid. The distance between windows in the IR flow cell was 0.1 mm. To avoid any particulate contamination leading to the cell blockage, a Pyrex glass filter with porosity $4-5.5$ μm was placed in the cell- feeding tubing. We chose quartz as a window material for our IR flow cell, since it is a sufficiently inert material. Some other IR- materials (ZnSe, CaF$_2$, Ge, and halides) were tested and were found to be less stable or more soluble in a highly aggressive ozone-containing reaction liquid. Quartz, as an optical material, has a sharp cutoff at $v < 2400$ cm^{-1}, at the same time water, which is the major component of the reaction mixture, blocked IR radiation at wavenumbers $v > 3000$ cm^{-1}. Thereby, this very narrow transmittance region ($2400 < v < 3000$ cm^{-1}) was used to determine dicarboxylic acid concentration using the peak in the area of $2550-2650$ cm^{-1}, which corresponds to the characteristic overtone frequency of the COOH group.

To obtain liquid-phase ozone concentrations we used calibration plots. These plots were obtained by measuring the gas-phase ozone concentration over an equilibrated water/ O$_3$ / O$_2$ mixture. The liquid-phase concentration was thereby calculated using the Henry's Law constant. We measured the absorbance of the liquid as a function of wavelength and acquired calibration plots from which we determined the concentration of dissolved ozone.

All dicarboxylic acids (99%) were received from Sigma- Aldrich (Canada). Extra dry oxygen (99.6%) was purchased from Matheson Tri-Gas (Canada). Molecular Sieves required for oxygen dryer (type 4A grade 514) were obtained from Fischer-Scientific.
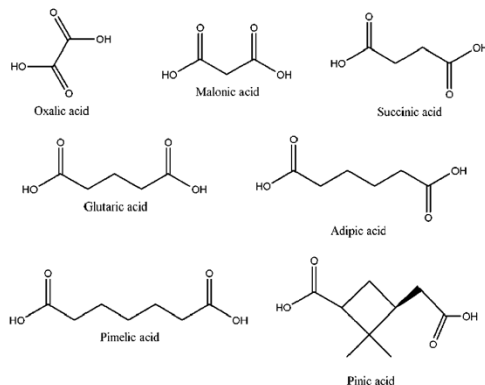

FIGURE 2. Chemical structures of studied dicarboxylic acids.

Results and Discussion

Ozonolysis of Dicarboxylic Acids. The reaction kinetics of the ozonolysis of selected dicarboxylic acids (C_2–C_9, see Figure 2) were investigated using two different techniques.

In the first method, we monitored the ozone concentration at a fixed dicarboxylic acid concentration. The dicarboxylic acid concentration was in excess relative to ozone so that the changes of dicarboxylic acid remained insignificant. In the second method, we monitored dicarboxylic acid decay at a fixed ozone concentration.

We performed 6–12 experiments for each compound. The results of both methods agreed within ±5% and are presented in Figure 3a,b. Aqueous solutions of dicarboxylic acids are typically observed in atmospheric aerosols of different composition (18). We chose concentrations in the range of 0.001–0.1 mol/L, where the upper limit has been approximately estimated from solubility of the studied carboxylic acids. Figure 3a illustrates that each dicarboxylic acid has a different reactivity toward ozone. By making observed concentration changes in a logarithmic format, we obtain straight lines for all of the dicarboxylic acids studied (see Figure 3c), demonstrating the second-order nature of these reactions

$$-\frac{d[DAC]}{dt} = -\frac{d[O_3]}{dt} = k[O_3] \cdot [DAC] \tag{1}$$

where k is the apparent reaction rate coefficient, t is time, and [DAC] as well as [O_3] represent dicarboxylic acid and ozone concentrations, respectively.

In dicarboxylic acid ozonolysis experiments using the ozone-decay method, ozone self-decomposition can be a problem, therefore decomposition rates at specific pH ranges (1.5–5.0) in various aqueous dicarboxylic acid solutions were measured. We observed that by increasing pH, the self-decomposition reaction rate increases as shown in Figure 3d. At higher pH (ca. 4.0–5.0), we noted that ozone self-decomposition rates under such conditions are comparable to the rates of ozonolysis of some of dicarboxylic acids. This may provide a partial explanation for certain over-estimations of ozonolysis rate constants of succinic and glutaric acids in previous studies (19). All the reported rate constants in this study have been corrected for the ozone self-decomposition reactions. The rate constants of dicarboxylic acid ozonolysis reactions are summarized and compared to literature, where available, in Table 1 (19).

As ozonolysis reactions proceed very slowly, in some experiments, ozone concentrations in the range of thousands to hundreds of ppmv (1 ppmv = 2.46×10^{13} molecule/cm^3) were used to shorten experiment times and reduce analytical errors associated with monitoring the dicarboxylic acid decay. However, this ozone concentration is far above of observed atmospheric concentrations of (0.01–0.1 ppmv) (20). To provide atmospherically relevant kinetic ozonolysis data, the dependence of dicarboxylic acid ozonolysis rates on ozone concentration were studied. As shown by in Figure 4a, ozonolysis rates vary linearly with ozone concentrations over a wide range, and hence the data can be extrapolated to atmospherically relevant concentrations.
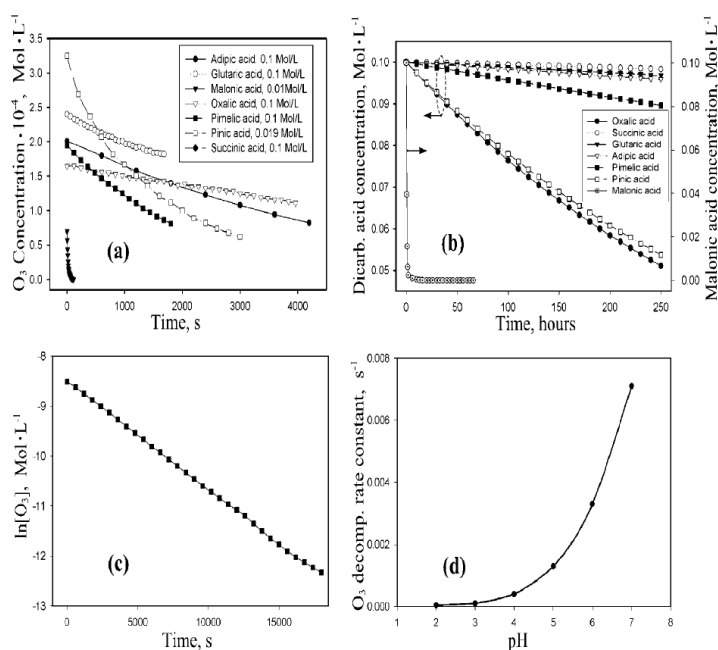

FIGURE 3. (a) Reactivity of dicarboxylic acids with ozone as a function of time at constant dicarboxylic acid concentration (method 1). (b) Reactivity of dicarboxylic acids with ozone at constant ozone concentration (method 2). (c) Adipic acid ozonolysis kinetics (0.1 mol L^{-1}) in logarithmic scale. (d) Ozone self-decomposition as a function of pH.

TABLE 1. Apparent Rate Constants of Ozonolysis and Photoassisted Ozonolysis of Selected Dicarboxylic Acids ($L \cdot mol^{-1} s^{-1}$)

dicarboxylic acid	ozonolysis rate constants[a] ($L \cdot mol^{-1} s^{-1}$)	photoassisted ozonolysis rate constants[a] ($L \cdot mol^{-1} s^{-1}$)	ozonolysis rate constants (ref 19) ($L \cdot mol^{-1} s^{-1}$)
oxalic	$(2.7 \pm 0.1) \times 10^{-2}$	$(3.0 \pm 0.2) \times 10^{-2}$	$2-4 \times 10^{-2}$
malonic	5.5 ± 0.1	5.9 ± 0.3	$4.0-7.0$
succinic	$(6.7 \pm 0.4) \times 10^{-4}$	$(8.1 \pm 0.8) \times 10^{-4}$	3.0×10^{-2}
glutaric	$(1.3 \pm 0.2) \times 10^{-3}$	$(1.5 \pm 0.1) \times 10^{-3}$	8.0×10^{-3}
adipic	$(1.7 \pm 0.1) \times 10^{-3}$	$(2.8 \pm 0.2) \times 10^{-3}$	no previous data
pimelic	$(4.4 \pm 0.1) \times 10^{-3}$	$(5.8 \pm 0.4) \times 10^{-3}$	no previous data
pinic	$(2.5 \pm 0.1) \times 10^{-2}$	$(2.9 \pm 0.2) \times 10^{-2}$	no previous data

[a] Uncertainties were calculated using t-error distribution: $k = k_{av} \pm t \cdot S$; where k is the value of the rate constant, k_{av} is an average value, t is the student's statistic coefficient for 95% confidence limit, and S represents standard deviation of measurements.

The most reactive dicarboxylic acid among the ones studied was malonic acid ($k = 5.5$ $Lmol^{-1}s^{-1}$). All other dicarboxylic acids were found to be $2-4$ orders of magnitude less reactive than malonic acid. Figure 4b depicts the dependence of dicarboxylic acid rate constants on the number of carbon atoms in a given dicarboxylic acid molecule. For longer chain dicarboxylic acids (C_n:n>3) reaction rate constants rise uniformly with increasing carbon number. This phenomenon is similar to that for aliphatic hydrocarbon ozonolysis (21), where an increase in the number of CH_2 groups in the molecule enhances the probability of ozone-CH_2 attack, leading to an increase in the rate constant. An empirical eq 2 that may be used for the estimation of ozonolysis rate constant for dicarboxylic acid (C_n; $n > 3$) with accuracy within $\pm 15\%$ ($R^2 = 0.97$) was derived

$$k = \exp(0.727 \times n - 10.392) \qquad (2)$$

where k is dicarboxylic acid ozonolysis rate constant, and n is the number of carbon atoms in the given dicarboxylic acid. The unit for this rate constant is $Lmol^{-1}s^{-1}$.

Interestingly, the first two members of homologous series of dicarboxylic acids, oxalic and malonic acids (C_2 and C_3), are exceptions to eq 2, since their ozonolysis reaction rates are 2 and 4 orders, respectively, higher in magnitude than predicted by the equation. This unusual behavior of oxalic and malonic acids is consistent with the difference in their ozonolysis reaction mechanism compared to the other dicarboxylic acids studied. As mentioned above, ozone may react with all long-chain dicarboxylic acids (C_n; $n > 3$) by CH_2-group attack (21), which results in low reaction rate constants. However, oxalic and, particularly, malonic acid are able to form cyclic (five- and six-center, respectively) transition molecule states with internal proton transfer from the carboxylic group to the carbonyl oxygen atom. This steric possibility exists only for oxalic and malonic acids and facilitates reactions such as acid decarboxylation. The malonic acid decarboxylation process involves an enol intermediate (22), which renders it an easy subject for decarboxylation. As shown in Figure 5, we suggest a similar type of reaction for the ozonolysis of malonic acid – the possibility of ozone attack on the carbon – carbon double bond (CdC). All other intermediate products, such as formaldehyde and formic acid, are also highly reactive with ozone ($k > 1 \times 10^2$ $Lmol^{-1}s^{-1}$) (19). The high stability of the six-centered transition state of malonic acid and the high reactivity of all its intermediates with ozone may explain the exceptionally high malonic acid ozonolysis rate constant.
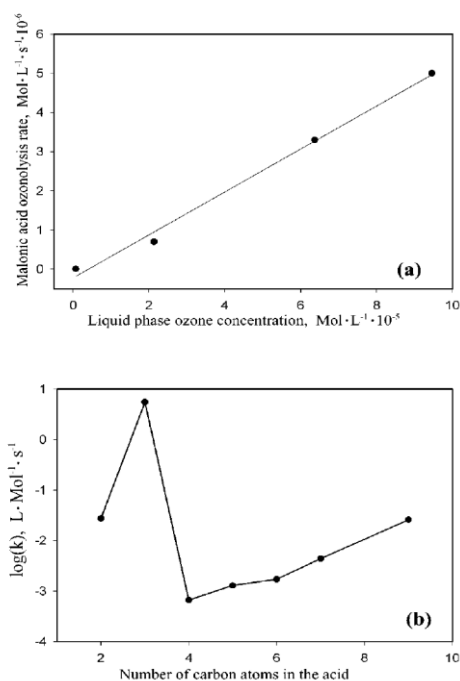
FIGURE 4. (a) Relationship between malonic acid ozonolysis reaction rate constant and ozone concentration in the liquid phase at 298 K; [HOOCCH$_2$COOH] = 0.01 mol·L^{-1}. (b) Dependence of ozonolysis rate constants and number of carbon atoms in dicarboxylic acids at 298 K.

Oxalic acid forms a five-center transition state, which promotes acid decarboxylationn through a similar mechanism as suggested for malonic acid. However, it should be noted that oxalic acid's five-center transition state is less stable than the six-centered structure of transition state of malonic acid, and this circumstance probably leads to lower oxalic acid ozonolysis rate constants relative to malonic acid. Notwithstanding, the oxalic acid ozonolysis rate constant is still exceptionally high compared to the rate constant values for other longer-chain dicarboxylic acids (C$_n$; $n > 3$).
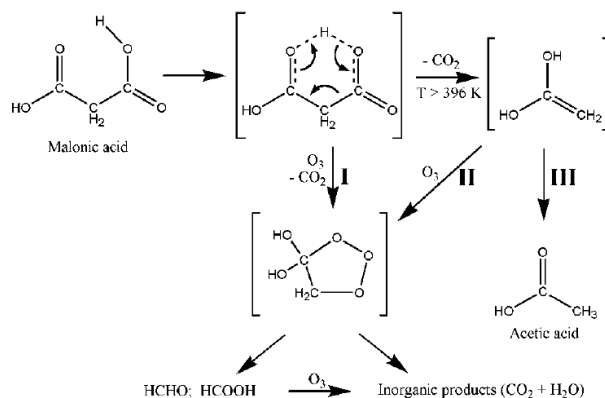

FIGURE 5. Malonic acid ozonolysis and decarboxylation reaction mechanisms: i. Reaction pathway in the presence of O$_3$ at $T < 396$ K. ii. Reaction pathway in the presence of O$_3$ at $T \geq 396$ K. iii. Reaction pathway in the absence of O$_3$ at $T \geq 396$.

TABLE 2. Lifetime of the Selected Dicarboxylic Acids upon Reactions with Atmospheric Oxidants

oxidant [X] dicarboxylic acids	reaction rate constants,[a] k (L·mol^{-1}·s^{-1})	lifetimes $\tau = 1/k[X]$ (days)	ref
HO• (aq)		(minimum)	(24)
oxalic	1.0×10^6	3.9	(25)
malonic	1.6×10^7	0.24	(26)
succinic	3.1×10^8	0.012	(27)
glutaric	8.3×10^8	0.005	(27)
adipic	2.0×10^9	0.002	(27)
pimelic	3.5×10^9	0.001	
HO$_2$• (aq)		>964	(28)
oxalic	<0.2	>643	(28)
malonic	<0.3	>771	(28)
succinic	<0.25		
O$_3$ (aq)	2.7×10^{-2}	428 669	
oxalic	5.5	2104	this study
malonic	6.7×10^{-4}	17 274 737	
succinic	1.3×10^{-3}	8 903 134	
glutaric	1.7×10^{-3}	6 808 279	
adipic	4.4×10^{-3}	2 630 471	
pimelic	2.5×10^{-2}	462 963	
pinic			

[a] Upper limits of aqueous [HO], [HO$_2$], and [O$_3$] of 3.0×10^{-12}, 6.0×10^{-8}, and 1.0×10^{-9} mol L^{-1}, respectively, were estimated using the Henry's law constants and gas-phase concentrations.

Photoassisted Ozonolysis. To sim ulate atmospheric aerosol conditions, ozonolysis reactions of the same dicarboxylic acids under UV ($\lambda \geq 250$ n m) exposure were studied. Similar to gas-phase chemistry, more complex kinetics of dicarboxylic acid degradation and higher reaction rates may be expected as the possibility for formation of radicals such as HO• exist (23), which is known to be a more reactive oxidant than ozone. We paid particular attention to study the reactions under conditions similar to those in atmospheric aerosols, including the measurement and comparison of solar and photolytic lamp spectra. However, we would like to caveat for potential differences between the reactions in the cell in this study and an atmospheric aerosol including the concentration of hydroxyl radical. Effective rate constants of the photoassisted ozonolysis of the dicarboxylic acids, as depicted in Table 1, were just slightly (10 −20%) higher than the corresponding "dark" ozonolysis rate constants under our experimental conditions. This may be explained by the so- called "cage" effect, which greatly reduces photochemical quantum yield of photolysis in solutions, com pared to the gas-phase photolysis (23). We attempted to estimate the dicarboxylic acid aerosols' lifetime in air, assuming an ozone mixing ratio of 100 ppbv, which is an upper limit for its summertime mid-latitude continental Northern Hemisphere values (20). In the case of malonic acid ozonolysis, which has the highest ozonolysis rate constant in this study, it takes years for 63% acid to be converted (lifetime), whereas for all other acids ozonolysis related conversion times are expected to be up to thousands of years.

In summary, a self-consistent data set of reaction rate constants for the ozonolysis of selected C$_2$−C$_9$ dicarboxylic acids, observed in atmospheric organic aerosols, was pro- vided. For prediction of unstudied dicarboxylic acid rate constants an empirical equation has been supplied. It has been shown that ozonolysis rate constants are dependent on the number of carbons in a given dicarboxylic acid. This is consistent with the increase in the possible ozone-CH$_2$ attacks. The surprisingly high rate constants for oxalic and malonic acids are attributed to the formation of five- and six- member ring intermediates. As shown in Table 2, a comparison of the lifetimes of dicarboxylic acids due to selected major atmospheric oxidants such as HO •(aq), HO$_2$•(aq), and O$_3$(aq) indicate that these reactions are too slow to be a major sink for dicarboxylic acids . It is thus established that ozonolysis and / or photolysis are not major sinks of dicarboxylic acids from the atmospheric aerosols.

Acknowledgments

Literature Cited

(1) Jacobson, M. C.; Hansson, H.-C.; Noone, K. J.; Charlson, R. J.*Rev. Geophys.* **2000**, *38*, 267−294.

(2) Glasius, M.; Lahaniati, M.; Calogirou, A.; Di Bella, D. et al.*Environ. Sci. Technol.* **2000**, *34*, 1001−1010.

(3) Kavouras, I. G.; Mihalopoulos, N.; Stephanou, E. G . *Environ. Sci. Technol*. **1999**, *33*, 1028−1037.

(4) Grosjean, D.; Friedlander, S. K. *Adv. Environ. Technol.* **1980**, *10*, 435.

(5) Schuetzle, D.; Cronn, D.; Crittenden, A. L.; Charlson, R. J. *Environ. Sci. Technol.* **1975** , *9*, 838.

(6) Cronn, D. R.; Charlson, R. J.; Knights, R. L.; Crittenden, A. L.; Appel, B. R. *Atmos. Environ.* **1977**, *11*, 929

(7) Yu, J.; Cocker, D. R.; Griffin, R. J.; Flagan, R. C.; Seinfeld, J. H. *J. Atmos. Chem.* **1999**, *34*, 207−258.

(8) Grosjean, D. *Secondary organic aerosols: identification and mechanisms of formation*; [Rep.] LBL (LBL-9037, Carbonaceous Part. Atmos.); Lawrence Berkeley Lab.: 1979; pp 107 −15.

(9) Novakov, T.; Corrigan, C. E. *Geophys. Res. Lett*. **1996**, *23*, 2141− 2144.

(10) Cronn, D. R. Ph.D. Dissertation, University of Washington: Seattle, 1975; 245 pp.

(11) Hatakeyama, S.; Ohno, M.; Weng, J.; Takagi, H.; Akimoto, H. *Environ. Sci. Technol*. **1987**, *21*, 52−57.

(12) Kawamura, K.; Usukura, K. *J. Oceanogr.* **1993**, *49*, 271−83.

(13) Kawamura, K.; Kasukabe, H.; Yasui, O.; Barrie, L. A. *Geophys. Res. Lett.* **1995**, *22*, 1253−6.

(14) Kawamura, K.; Semere, R.; Imai, Y.; Fujii, Y.; Hayashi, M. *J. Geophys. Res. [Atmos.]* **1996**, *101*, 18721−18728.

(15) Kawamura, K.; Sakaguchi, F. *J. Geophys. Res., [Atmos.]* **1999**, *104*, 3501−3509.

(16) Ansari, A. S.; Pandis, S. N. *Environ. Sci. Technol*. **2000**, *34*, 71− 77.

(17) Graedel, T. E.; Weschler, C. J. *Rev. Geophys. Space Phys*. **1981**, *19*, 505−39.

(18) Lightstone, J. M.; Onasch, T. B.; Imre, D.; Oatis, S. *J. Phys. Chem. A* **2000**, *104*, 9337−9346.

(19) Hoigne, J.; Barder, H. *Water Res*. **1983**, *17*, 185−194.

(20) Kelly, N. A.; Wolff, G. T.; Ferman, M. A. *Atmos. Environ*. **1982**, *16*, 1077−88.

(21) Bailey, P. S. *Ozonolysis in organic chemistry*; Academic Press: New York, 1978; Vol. 2.

(22) Loudon, G. M. *Organic chemistry,* 3rd ed.; Benjamin/Cummings Publishing Co. Inc.: Prude University, 1995.

(23) Walhout, P. K.; Silva, C.; Barbara, P. F. *J. Phys. Chem*. **1996**, *100*, 5188−99.

(24) Getoff, N.; Schwoerer, F.; Markovic, V. M.; Sehested, K.; Nielsen, S. O. *J. Phys. Chem*. **1971**, *75*, 749−55.

(25) Walling, C.; El-Taliawi, G. M. *J. Am. Chem. Soc.* **1973**, *95*, 844.

(26) Cabelli, D. E.; Bielski, B. H. J. Z. *Naturforsch., B, Anorg. Chem., Org. Chem.* **1985**, *40B*, 1731−7.

(27) Scholes, G.; Willson, R. L. *Trans. Faraday Soc*. **1967**, *63*, 2983− 93.

(28) Bielski, B. H. J.; Richter, H. W. *J. Am. Chem. Soc.* **1977**, *99*, 3019− 23.